Geophysical Research Letters

RESEARCH LETTER
10.1029/2025GL117096

Drought-Induced Land Subsidence in the Mekong Delta, Vietnam: Insights From SAR Interferometry

Nils Dörr[1], **Long Vu Huu**[1,2], **Andreas Schenk**[1], **and Stefan Hinz**[1]

[1]Institute of Photogrammetry and Remote Sensing, Karlsruhe Institute of Technology, Karlsruhe, Germany, [2]Vietnam National Space Center (VNSC), Vietnam Academy of Science and Technology (VAST), Hanoi, Vietnam

Abstract The Mekong Delta has been affected by land subsidence for decades, increasing its vulnerability to coastal erosion and floodings. Here we show, based on subsidence time series from SAR Interferometry, that severe droughts can significantly intensify the subsidence. We measured a subsidence of up to 7 cm in few months during a drought in 2020, which was compensated by uplift in the following rainy season in some but not all regions. The magnitude of the drought-induced subsidence was spatially correlated with specific surface water management and land use zones, with the largest impact in rain-fed, rice growing regions. We argue that the uncompensated surface drop in two regions, reaching up to 3.5 cm, was caused by inelastic deformation. Such irreversible subsidence has a major impact on the delta's future elevation, especially under the assumption that the frequency of droughts will increase under climate change and an increasing water demand.

Plain Language Summary The sinking of land, known as land subsidence, increases the sea-level rise in coastal areas. The Mekong Delta has been affected by such subsidence for more than 2 decades, making it increasingly vulnerable to floodings and land loss. Based on measurements from satellite radar remote sensing, our research shows a so far unknown driver of subsidence in the delta. A severe drought in 2020 led to significant short-term sinking of the delta, which added to the long-term subsidence trend. We found that its magnitude was spatially correlated with surface water management zones and the land use. Furthermore, we argue that the exceptional subsidence in two coastal regions was partly irreversible. Consequently, droughts considerably intensify the problem of the relative sea level rise in the Mekong Delta, which is of increasing concern since droughts become more frequent as a result of climate change.

Key Points:

- A severe drought in 2020 caused subsidence of up to 7 cm in few months in the Mekong Delta, adding up to the background subsidence trend
- We observed a permanent ground surface drop of up to 3.5 cm, which we argue was caused by inelastic deformation
- The magnitude of the drought-induced subsidence was spatially correlated with specific surface water management zones and land use types

Correspondence to:
N. Dörr,
nils.doerr@kit.edu

Citation:
Dörr, N., Huu, L. V., Schenk, A., & Hinz, S. (2025). Drought-induced land subsidence in the Mekong Delta, Vietnam: Insights from SAR Interferometry. *Geophysical Research Letters*, *52*, e2025GL117096. https://doi.org/10.1029/2025GL117096

Received 21 MAY 2025
Accepted 13 SEP 2025

Author Contributions:
Conceptualization: Nils Dörr, Long Vu Huu, Andreas Schenk
Formal analysis: Nils Dörr
Investigation: Nils Dörr
Methodology: Nils Dörr, Long Vu Huu, Andreas Schenk
Visualization: Nils Dörr
Writing – original draft: Nils Dörr
Writing – review & editing: Nils Dörr, Andreas Schenk, Stefan Hinz

1. Introduction

Land subsidence poses a great threat to river deltas, which host more than 500 Million people worldwide (Anthony et al., 2024; Syvitski et al., 2009), increasing their vulnerability to salinization of water resources (Don et al., 2006; Smajgl et al., 2015), flooding (Miller & Shirzaei, 2019; Tellman et al., 2021), coastal erosion (Zou et al., 2016), and permanent inundation. The Mekong Delta, lying at an average elevation of 0.8 m above sea level (Minderhoud et al., 2019), has been affected by subsidence for more than 15 years, with rates that reach 7 cm/yr (Dörr et al., 2024a; Erban et al., 2014; Minderhoud, Hlavacova, et al., 2020). Investigating the causes of the subsidence is crucial for the development of reasonable countermeasures and adaptations, which are needed to prevent the projected future drowning of parts of the delta (Kondolf et al., 2022; Minderhoud, Middelkoop, et al., 2020).

The subsidence in the Mekong Delta has mainly been attributed to groundwater over-exploitation (Erban et al., 2014; Karlsrud et al., 2020; Minderhoud et al., 2017), and natural compaction of Holocene clays (Baldan et al., 2024; Zoccarato et al., 2018). The new availability of recent subsidence time series across the delta by Dörr et al. (2024a) enables deeper insights into the origins of the subsidence, by enabling the analysis of inter-annual and short-term deviations from linear subsidence. They showed the presence of significant temporal non-linearities and seasonal variations at various locations in the delta. The rapid subsidence at two locations during a severe drought in 2020 was particularly striking. During the same drought, various news reports in Vietnam described that water channels in the Mekong Delta completely dried up, and that bridges, roads, and dykes collapsed into such channels.

In this work, we use openly available land subsidence measurements over the Mekong Delta, derived from Sentinel-1 Interferometric Synthetic Aperture Radar (InSAR), to study the relationship between seasonal variations in the subsidence, dryness conditions, land use and surface water management. A main focus is laid on the

10.1029/2025GL117096

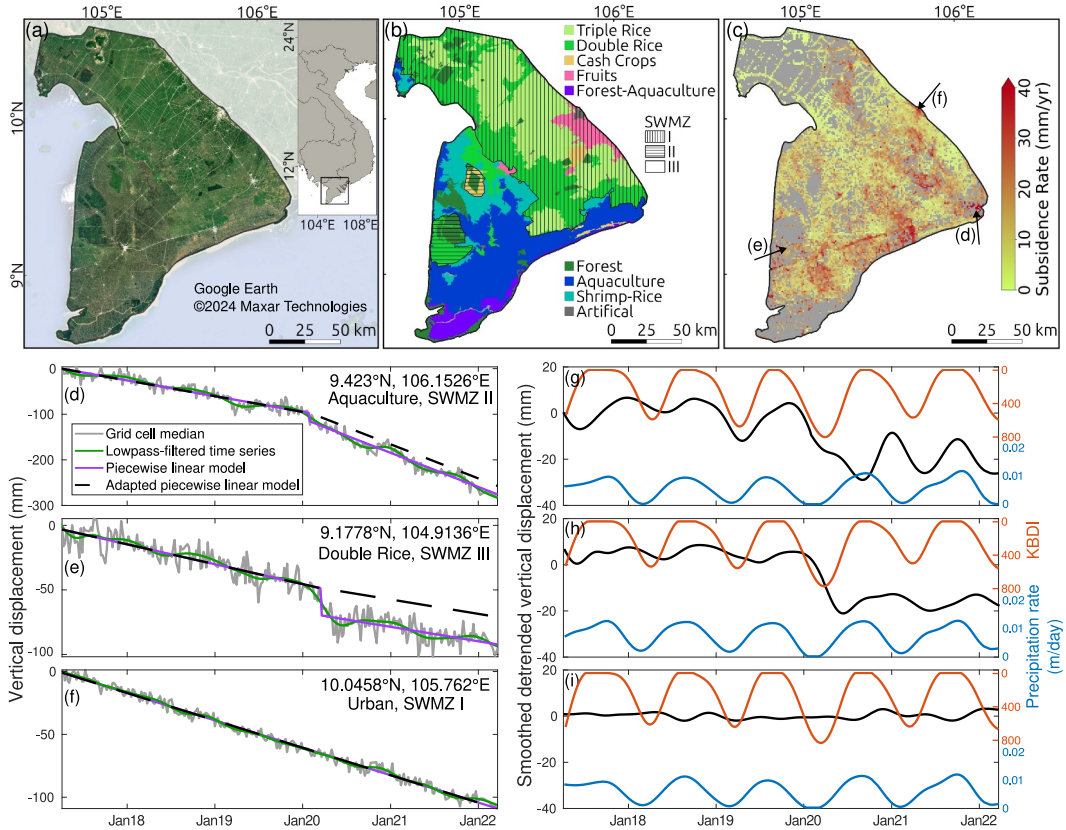

Figure 1. (a) Satellite image composite of the Mekong Delta from Google Earth, © Maxar Technologies. The study area south-west of the Hau River is indicated by full opacity. (b) Land use classification from Berchoux et al. (2023), overlaid by the surface water management zones. (c) Subsidence rates between 2017 and 2022 from Dörr et al. (2024b), resampled with a median filter to a 1×1 km grid. (d–f) Median time series and processing results of vertical displacements within three exemplary grid cells. (g–i) Smoothed detrended vertical displacement time series, as well as Keetch-Byram Drought Index and precipitation rate time series, which were smoothed the same way as the subsidence time series.

identification and analysis of the rapid subsidence event during the 2020 drought, which amounted up to several centimeters in few months in parts of the delta, and added to the background subsidence trend.

2. Study Area

The Mekong Delta (Figure 1) was built up through a stratification of marine and alluvial deposits from the Miocene and Holocene, which form seven confined aquifers and aquitards (Wagner et al., 2012). It has a tropical monsoon climate which features a rainy season from May to October and a dry season in the rest of the year (Bui et al., 2017; Kumiko et al., 2008). The frequency of droughts has increased in the last 30 years, with the most extreme droughts recorded in 2016 and 2020 (Loc, Van Binh, et al., 2021; Trung et al., 2021). They can lead to significant rice crop failures (Lavane et al., 2023) and a salinity intrusion into surface waters (Kaveney et al., 2023; Loc, Van Binh, et al., 2021).

The complex land use system in the study area, mainly consisting of rice, aquaculture, and shrimp-rice rotational crops (Loc, Low Lixian, et al., 2021; Mills et al., 2023), is linked to a complex water management system. While the dense channel and hydraulic control system was originally built to provide freshwater zones for rice production across the delta (Käkönen, 2008), the various farming practices today require different surface water salinity contents and management systems. In Figure 1b, we roughly distinguish between three surface water management zones (SWMZs), whose classification is adapted from Wehrheim et al. (2023). SWMZ I is a freshwater zone, which is always hydraulically connected to the Mekong river and protected from saltwater intrusion during dry seasons by sluice gates. SWMZ II describes managed rain-fed freshwater zones of the Lower and Upper U Minh forests and surroundings, which are used for rice and cash crop cultivation. They are bordered

by sluice gates to the surrounding SWMZ III, which comprises the remaining brackish/saline regions that are mainly used for aquaculture and shrimp-rice rotational crops. Parts of this zone are fed by the river in rainy seasons, whereas the whole zone is disconnected from SWMZ I during dry seasons. The location-dependent water management in SWMZ III probably relies on the season and specific land use. We assume that areas of pure rice cultivation in SWMZ III are closed off with sluice gates from surrounding areas during dry seasons to prevent a salinity intrusion.

3. Material and Methods

3.1. Land Subsidence Observations

We utilized Sentinel-1 InSAR derived subsidence time series which were described in Dörr et al. (2024a) and published in Dörr et al. (2024b). We used the results of the descending orbit stack, covering the period between April 2017 and April 2022, and applied three processing steps to (a) remove isolated movements and resample the subsidence data to a regular spatial grid, (b) filter out spatially correlated high-frequency signals, and (c) remove the background subsidence trend.

The first step was realized by calculating the median subsidence time series of measurement points within grid cells of 1×1 km size. The second step was achieved by applying a Butterworth filter with a cutoff frequency of 2/yr, in order to robustly remove high-frequency signals while retaining seasonal movements. For the last step, we removed an adapted piecewise linear model from the smoothed time series, which was estimated in a two-step process. First, a piecewise linear model was estimated with an iterative change point detection approach that separates linear segments with deviating slopes. Discontinuous steps between linear segments, which we attribute to seasonal variations of interest instead of the background subsidence trend, were then removed to derive the adapted piecewise linear model. Examples of the time series processing steps are shown in Figure 1. The displayed grid cells are located in different land use zones and SWMZs, and were selected in such a way that the removal of the background trend is illustrated for different land subsidence patterns.

3.2. Meteorological Information

We utilized the Keetch-Byram Drought Index (KBDI) (Keetch & Byram, 1968) and precipitation time series from the ERA-5 Land archive, both available at the Google Earth Engine database (Muñoz Sabater et al., 2024; Takeuchi et al., 2015), to characterize temporal variations in dryness during the subsidence observation period. The KBDI is a meteorological drought index based on daily maximum temperatures and cumulative rainfall data, representing the balance between water loss through evaporation and water gain from precipitation. Therefore, it is particularly useful to describe regions where rainfall is the primary means of soil moisture replenishment. It is widely used in fire management practices (Brown et al., 2021; Yoon et al., 2015) and drought monitoring in agriculture (Takeuchi et al., 2015). The KBDI's scale from 0 to 800 indicates increasing levels of moisture deficiency.

We accumulated the precipitation that occurred between individual acquisitions of the subsidence data set, to derive a time series with the same temporal sampling as the subsidence data. For the seasonal displacement prediction (Section 3.3), we divided the precipitation data at each time instance by the time difference to the previous instance, to derive an average precipitation rate per day. Examples of KBDI and precipitation rate time series, which were smoothed the same way as the subsidence time series, are displayed in Figure 1.

3.3. Seasonal Displacement Prediction

We conducted a linear regression analysis to study the potential of predicting seasonal vertical displacements using KBDI and/or precipitation rate as predictors. The regression estimated the linear relationship between the predictors and the instantaneous seasonal displacement rate, which we then integrated to receive displacement time series. We found that the parameter estimation for the regression worked best when predicting smoothed seasonal vertical displacements with predictors which were smoothed in the same way. Negative values in the smoothed predictor time series were set to 0.

A preliminary test showed a distinct multicollinearity for a regression with both KBDI and precipitation rate as predictors, hence we only studied separate regressions in the following. As the prediction with precipitation consistently delivered better results than the one with KBDI, we only show the results of the former here. The regression model parameters were estimated based on the time prior to the drought in 2020, characterizing

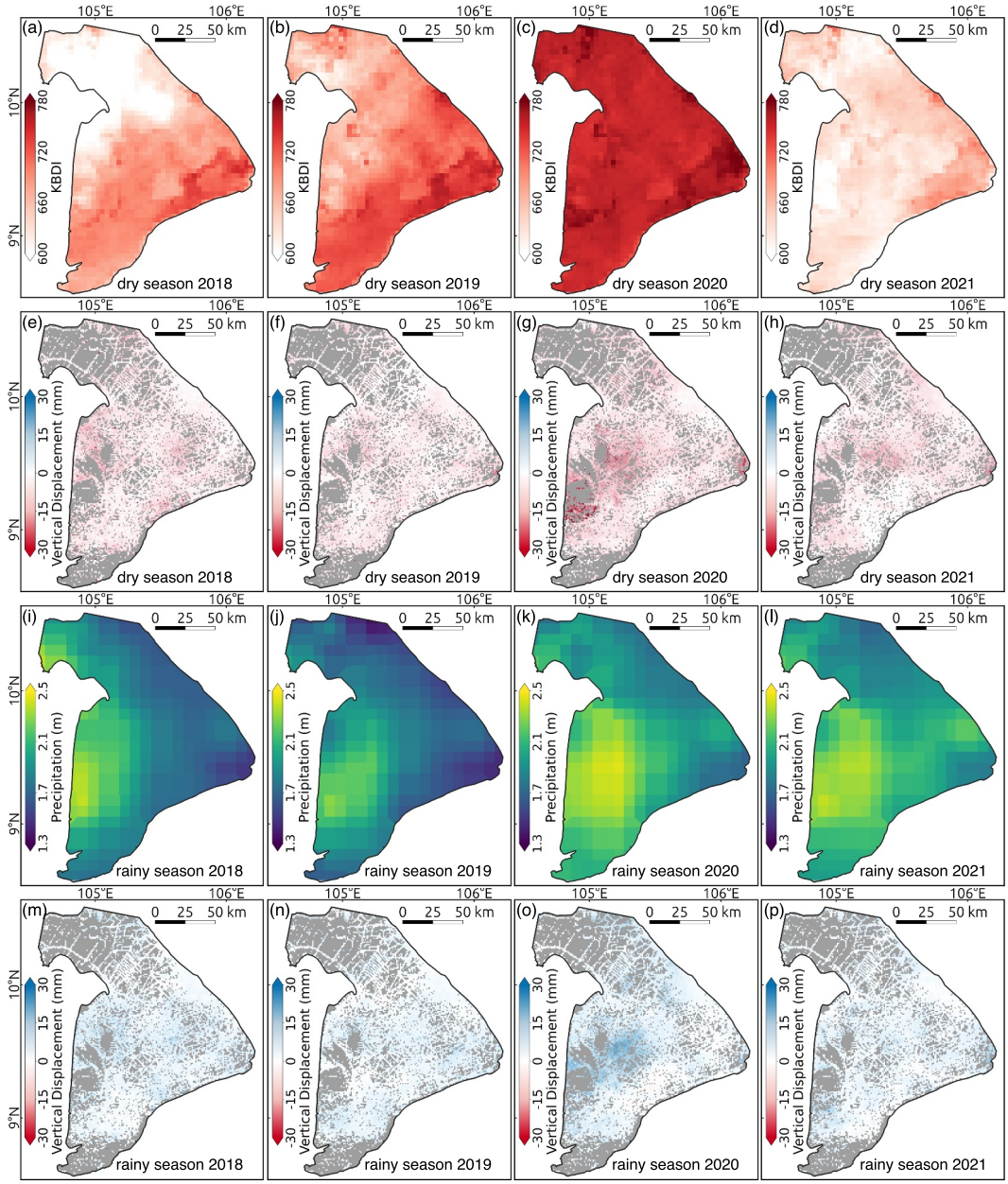

Figure 2. (a–d) Ninety-five percent percentile of Keetch-Byram Drought Index values in dry seasons, which last from November of the previous year to May of the given year. (e–h) Accumulated vertical displacements in dry seasons, extracted from the smoothed seasonal displacement time series. Positive and negative values represent uplift and subsidence, respectively. (i–l) Precipitation sum in rainy seasons. (m–p) Same as (e–h) for rainy seasons.

undisturbed seasonal conditions. With the set up regression model, four different time series segments were predicted: before the 2020 drought (November 2017–November 2019), during the drought (May 2019–May 2021), after the drought (May 2020–April 2022), and the whole time series.

4. Results

4.1. Seasonal Vertical Displacements

The drought in 2020 was preceded by increasing peak KBDI values in the two previous dry seasons (Figure 2). During the drought, the largest KBDI values of up to 780 were identified, inter alia, in SWMZ II and the Hau river

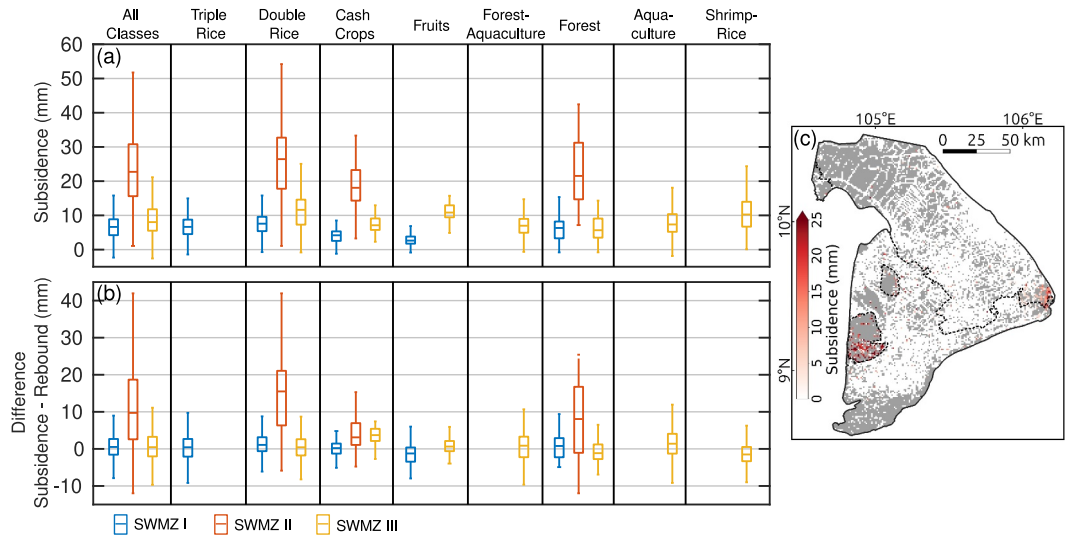

Figure 3. (a) Boxplots of the total seasonal subsidence during the drought in 2020, with respect to the surface water management zones and land use. (b) Boxplots of the differences between the seasonal subsidence and uplift during the drought and following rainy season in 2020, respectively. No outliers are displayed in any of the boxplots. (c) Detected permanent ground surface drop during the drought.

estuaries. In each rainy season, the precipitation sum exhibited the highest values in the western part of the study area. The overall precipitation sum in the rainy season of 2020 was larger than in the previous years, leading to an end of the drought and comparably low KBDI values in the following dry season.

The seasonal vertical displacement of two of the three example time series in Figure 1 showed seasonal undulations, with subsidence and uplift during the dry and rainy seasons, respectively. Across the delta, the magnitude of such seasonal subsidence and uplift varied in time and space (Figure 2). Particularly high seasonal subsidence occurred in parts of the delta during the drought in 2020. This especially affected the southern part of SWMZ II, where a seasonal subsidence of up to 70 mm was identified. The boundary of this affected area aligns precisely with the boundary of the southern SWMZ II. Other areas with high seasonal subsidence during the drought were in and around the northern part of SWMZ II as well as the areas around the Hau river estuary, where the subsidence reached up to 36 and 40 mm, respectively. The uplift in the following rainy season was also partly larger than the uplift in the other rainy seasons. In the areas around the northern part of SWMZ II, where the maximum precipitation sum was identified, the uplift was comparable to the preceding subsidence. The exceptional subsidence in the southern part of SWMZ II and around the Hau river estuary was not compensated by the ensuing uplift at most pixels.

Statistics of the seasonal subsidence during the 2020 drought, broken down by SWMZs and land use classes, are displayed in Figure 3a.

The highest average seasonal subsidence occurred in SWMZ II with a median of 23 mm, while the medians in SWMZs I and III were 7 and 8 mm, respectively. In relation to land use classes, we identified the largest values in the double rice areas in SWMZ II, where the 50% and 95% percentiles of the seasonal subsidence were 26 and 47 mm, respectively. In SWMZ I, the median seasonal subsidence was below 10 mm in all land use classes, whereas the double rice, fruits, and shrimp-rice areas in SWMZ III were affected by a slightly larger median than 10 mm.

The seasonal subsidence, which occurred in SWMZs I and III during the drought in 2020, was compensated, on average, by a rebound in the following rainy season (Figure 3b). This did not apply to SWMZ II, where the median rebound deficit was 10 mm. The most significant deficits in that zone were found in the double rice and forest areas, with median differences of 16 and 8 mm, respectively. The magnitude of these differences agrees with the magnitude of the ground surface drops, which were identified by the adapted piecewise linear model during the drought in 2020 (Figure 3c). They reached up to 35 mm in SWMZ II and 27 mm in the Hau river estuaries.

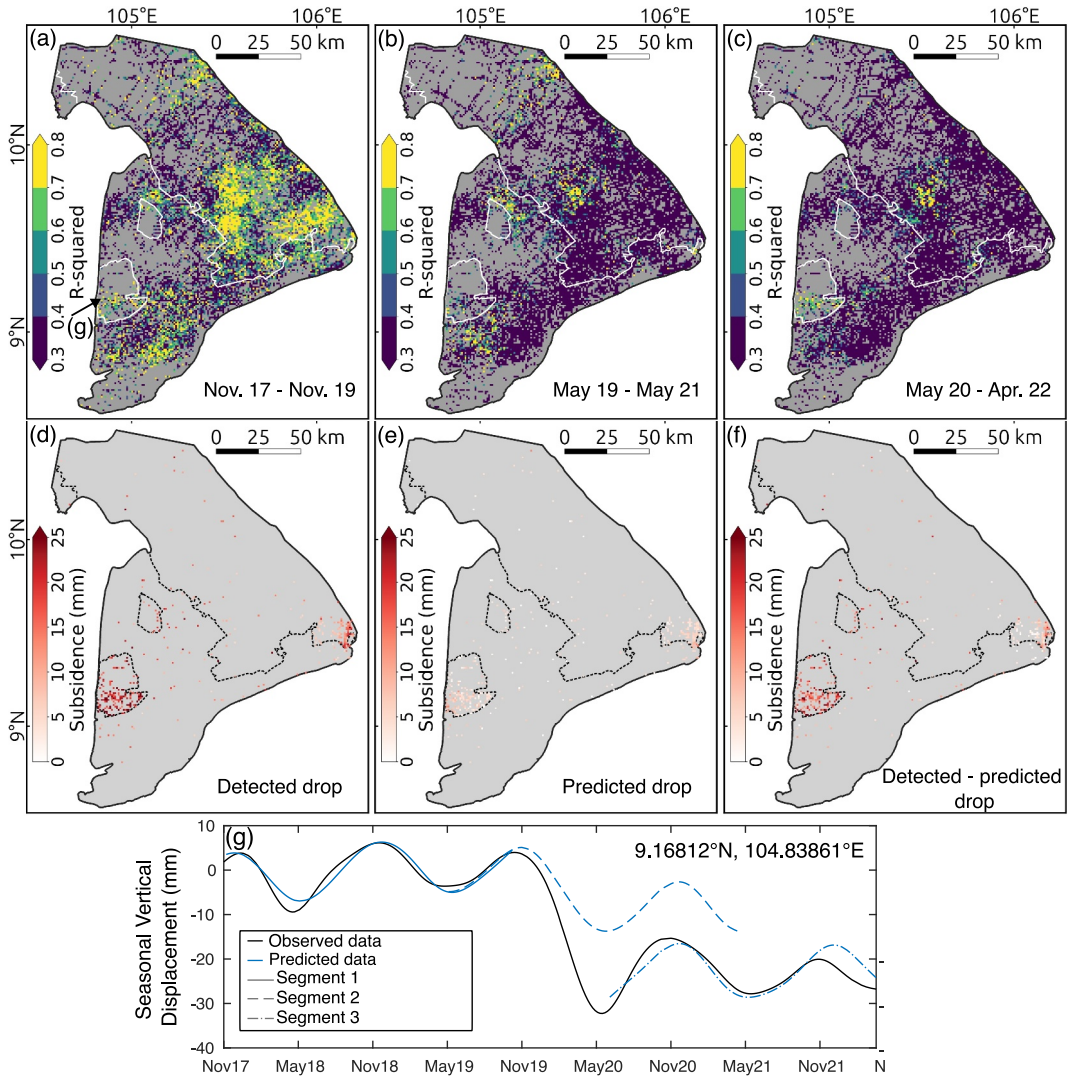

Figure 4. (a–c) *R*-squared measure for the prediction of the seasonal displacement in three time segments with precipitation. Only pixels which passed the Overall-F-Test for the prediction of the first segment are displayed. (d, e) Detected and predicted ground drop during the drought in 2020. (f) Difference between (d) and (e). (g) Example time series with prediction. The location is indicated by the arrow in panel (a).

4.2. Seasonal Displacement Prediction

The *R*-squared measure for the precipitation-based prediction of the seasonal vertical displacements in the three temporal sub-segments is displayed in Figure 4.

It shows a large spatial heterogeneity for the first segment, with 5% and 95% percentiles of 0.08 and 0.83, respectively. The largest values were found in the southern part of SWMZ I, but there were also high values in and around SWMZ II, as well as in the southern part of SWMZ III. The values decreased significantly from the first to the last segment at most locations. One of few exceptions is the lower SWMZ II, where the *R*-squared measure decreased considerably from the first to the second segment, while it increased again in the last segment, reaching values of over 0.8. This is also visible in the exemplary time series in Figure 4g. The large ground surface drop in the second segment could not be predicted reasonably, but the prediction showed reasonable performance in the first and last segment.

By predicting the whole available time series, we could study the potential to predict the observed ground drops during the 2020 drought. The drop was computed by means of the piecewise linear model, as for the measured

data. The results are displayed in Figures 4e and 4f for pixels with a detected drop in the measured displacement time series. The regression model was not capable of predicting the whole observed surface drop at most locations. The mean of the predicted and unpredicted drops was 5.4 and 18.1 mm, respectively, in the southern part of SWMZ II. The ground surface drop at strongly affected grid cells in the Hau river estuaries could also not be predicted reasonably.

5. Discussion and Conclusions

We here analyzed InSAR-derived subsidence time series at measurement points, which were mainly located on man-made structures that might have foundations in different depths. Consequently, their measured movements reflect various shares of the total land subsidence and might additionally contain loading-induced subsidence, as discussed in de Wit et al. (2021), Dörr et al. (2021), and Minderhoud et al. (2025). We aggregated point measurements within 1×1 km grid cells, which might cause different cells to reflect subsidence in various depth ranges, depending on the sampled structures inside the cells. However, we assume that foundations are mostly shallow in rural, agricultural areas like SWMZ II, so most measurement points reflect the largest part of the total subsidence. We attempted to suppress isolated movements of individual buildings, due to large loads, largely deviating foundation depths from grid cell averages and construction-related tilting, by using the median for aggregation.

We found that various locations across the Mekong Delta are affected by a subsidence which is the sum of a background trend overlaid by seasonal vertical displacements in phase with the dry and rainy seasons. The observed background trend is assumed to be the result of groundwater over-exploitation and natural compaction of Holocene clay sediments (Baldan et al., 2024; Minderhoud et al., 2017). The overlaying seasonal displacements reflect a system component, in which subsidence due to water scarcity in the dry seasons is decelerated, or partially or completely compensated by a rebound in the rainy seasons. The seasonal signals might be related to a seasonality in the groundwater extraction rates, resulting in a seasonally varying compaction of the aquifer-aquitard system (Bell et al., 2008; Haghighi & Motagh, 2024), as well as to drying and wetting related shrinkage and swelling of shallow clayey soils (Stewart et al., 2016). In general, our remote sensing based approach is not able to clarify to what extent the mechanisms behind the background and seasonal signals are coupled, hence to which extend the observed seasonal variations are elastic or inelastic.

Parts of the study area were affected by extraordinary subsidence of up to 7 cm in few months during the severe drought in 2020. The magnitude was clearly spatially correlated with specific surface water management and land use zones. Strongly affected areas were also characterized by particularly large KBDI values during the drought, probably induced by large land surface temperatures. The largest subsidence was found in rain-fed double-rice agricultural areas in SWMZ II around the Lower U Minh forest. At this location, the median of the seasonal subsidence during the drought, neglecting the background subsidence, was 23 mm. Other strongly affected areas were double-rice and shrimp-rice areas around the northern part of SWMZ II, which are probably also not hydraulically connected to the Hau river during dry seasons, as well as aquaculture and double-rice areas around the Hau river estuary. Those areas were also characterized by very large peak KBDI values. Most other areas in SWMZ III and SWMZ I were not affected by unusual subsidence.

There are two possible reasons for the observed drought-induced subsidence. First, the groundwater extraction rates might have been significantly increased during the drought, to meet the needs of the land use and domestic water usage (Van Loon et al., 2016). Freshwater in the double-rice areas in SWMZs II and III is only supplied by rain or groundwater. The increased salinity and evaporation in the brackish/saline zones during the drought could also have been a reason for increased groundwater extraction rates in aquaculture areas in SWMZ III. Fresh groundwater might be mixed with saline surface waters to keep the salinity for shrimp growth at a reasonable level. Land subsidence, originating from aquifer-aquitard compaction due to groundwater over-extraction which intensified during droughts, has been reported for the Central Valley in California by Ojha et al. (2018), Chaussard et al. (2017), and Miller et al. (2020), where the latter measured a peak cumulative subsidence of roughly 90 cm during a severe drought between 2014 and 2017. The second reason could be an exceptional drying of the surface sediments, leading to soil shrinkage in clayey soils. This effect would probably be mostly relevant to the rain-fed only zones in SWMZs II and III. SWMZ I has an all-year hydraulic connection to the Mekong river, leading to a less pronounced freshwater scarcity during droughts, hence probably to a smaller deviation of the groundwater extraction rates and soil moisture from normal dry seasons compared to SWMZs II and III. Overall,

our remote sensing observations do not allow us to determine how much each mechanism contributed to the drought-induced subsidence.

The seasonal subsidence during the drought in 2020 was not compensated by uplift in the following rainy season in the southern part of SWMZ II and around the Hau river estuary. In the southern SWMZ II, the detected ground surface drop reached up to 35 mm and its median value was 17.5 mm. This drop could either be caused by a permanently lowered water table, or by inelastic subsidence. While the precipitation sums in the two rainy seasons after the drought were higher than in the 2 years before, the ground surface level was not characterized by an uplifting trend. This indicates that the first mentioned reason appears unable to explain the sudden inability to compensate the subsidence. Inelastic subsidence could have been originating in the aquifer-aquitard system, or been caused by inelastic shallow soil subsidence in response to a significant moisture loss, which also could have led to reported collapses of roads and dykes into nearby channels. Welch et al. (2024) reported such inelastic subsidence in clayey soils of up to 8 mm during recent droughts at the coast of Texas, USA, amounting to roughly 10% of the total subsidence. Regardless of the cause, the observed drop indicates a deviation of the hydrogeological system from its normal state in the other studied years.

These findings were supported by our seasonal displacement prediction analysis. The subsidence prediction by means of precipitation data is not capable of deciphering the underlying mechanisms, but we assume low-pass filtered precipitation to act as a proxy in the rain-fed zones, primarily for changes in groundwater extraction rates and soil moisture. The prediction showed good performance in the southern SWMZ II for temporal segments without drought conditions, while the model was unable to predict the subsidence during the drought. This contrasting performance underlines the hypothesis that the hydrogeological system deviated from its normal state during the drought. The good prediction capabilities in other seasons, using precipitation as the predictor variable, aligns with the fact that the surface water input in this area is neither impacted by the river nor the sea. The overall prediction performance was not adequate in other regions which were affected by seasonal displacements. In general, hydrogeological models which incorporate groundwater extraction rates and pressure heads in different aquifers, the water table depth and soil moisture are required for reasonable subsidence predictions, which allow an explanation of the underlying mechanisms. Longer subsidence time series which span several years without and with severe drought conditions would also help to set up more robust displacement models.

This study showed that droughts can significantly intensify land subsidence in the Mekong Delta, and drought-induced subsidence in 2020 was spatially correlated with specific surface water management and land use zones. The potential irreversible subsidence during droughts has a major impact on the low-lying delta, especially under the assumption that the frequency of droughts will increase due to climate change and an increasing water demand. Studying the underlying mechanisms of the observed drought-induced subsidence is subject to future research, which preferably considers the actual hydrogeology and bases on longer subsidence time series in combination with measurements from monitoring stations which measure depth-dependent subsidence, aquifer pressure heads, water table depth, and soil moisture.

Acknowledgments
All figures with geographical context have been produced with the QGIS software. We thank Felix Dörr and Jonas Bauer from the Institute of Applied Geosciences at the Karlsruhe Institute of Technology for fruitful discussions. We also thank Tristan Berchoux from CIHEAM-Montpellier for providing the land use classification used in this research. We are thankful for constructive and helpful comments by Philip Minderhoud and one anonymous reviewer, which helped to improve the manuscript. The preparational work of this research was conducted in the frame of the ViWaT Engineering project, which was funded by the German Ministry for Education and Research (BMBF). We acknowledge support by the KIT Publication Fund of the Karlsruhe Institute of Technology. Open Access funding enabled and organized by Projekt DEAL.

Conflict of Interest

The authors declare no conflicts of interest relevant to this study.

Data Availability Statement

The InSAR-derived subsidence data from Dörr et al. (2024b) is publicly available at https://radar.kit.edu/radar/en/dataset/YYpQiWnfZaqMVybS, the KBDI data (Takeuchi et al., 2015) is available via Google Earth Engine at https://developers.google.com/earth-engine/datasets/catalog/UTOKYO_WTLAB_KBDI_v1, and the ERA-5 reanalysis based precipitation data from Muñoz Sabater et al. (2024) can be accessed from the Google Earth Engine at https://developers.google.com/earth-engine/datasets/catalog/ECMWF_ERA5_DAILY.

References

Anthony, E., Syvitski, J., Săinescu, F., Nicholls, R. J., Cohen, K. M., Marriner, N., et al. (2024). Delta sustainability from the Holocene to the Anthropocene and envisioning the future. *Nature Sustainability*, *7*(October), 1235–1246. https://doi.org/10.1038/s41893-024-01426-3

Baldan, S., Minderhoud, P. S. J., Xotta, R., Zoccarato, C., & Teatini, P. (2024). Data-driven 3D modelling of long-term Holocene delta evolution and sediment compaction: The Mekong Delta. *Earth Surface Processes and Landforms*, *50*(1), 1–14. https://doi.org/10.1002/esp.6046

Bell, J. W., Amelung, F., Ferretti, A., Bianchi, M., & Novali, F. (2008). Permanent scatterer InSAR reveals seasonal and long-term aquifer-system response to groundwater pumping and artificial recharge. *Water Resources Research*, *44*(2), 1–18. https://doi.org/10.1029/2007WR006152

Berchoux, T., Hutton, C. W., Hensengerth, O., Voepel, H. E., Tri, V. P., Vu, P. T., et al. (2023). Effect of planning policies on land use dynamics and livelihood opportunities under global environmental change: Evidence from the Mekong Delta. *Land Use Policy*, *131*(May), 106752. https://doi.org/10.1016/j.landusepol.2023.106752

Brown, E. K., Wang, J., & Feng, Y. (2021). US wildfire potential: A historical view and future projection using high-resolution climate data. *Environmental Research Letters*, *16*(3), 034060. https://doi.org/10.1088/1748-9326/aba868

Bui, D. D., Nguyen, N. C., Bui, N. T., Le, A. T. T., & Le, D. T. (2017). Climate change and groundwater resources in Mekong Delta, Vietnam. *Journal of Groundwater Science and Engineering*, *5*(1), 76–90. https://doi.org/10.26599/JGSE.2017.9280008

Chaussard, E., Milillo, P., Bürgmann, R., Perissin, D., Fielding, E. J., & Baker, B. (2017). Remote sensing of ground deformation for monitoring groundwater management practices: Application to the Santa Clara valley during the 2012–2015 California drought. *Journal of Geophysical Research: Solid Earth*, *122*(10), 8566–8582. https://doi.org/10.1002/2017JB014676

de Wit, K., Lexmond, B. R., Stouthamer, E., Neussner, O., Dörr, N., Schenk, A., & Minderhoud, P. S. (2021). Identifying causes of urban differential subsidence in the Vietnamese Mekong Delta by combining InSAR and field observations. *Remote Sensing*, *13*(2), 1–33. https://doi.org/10.3390/rs13020189

Don, N. C., Hang, N. T. M., Araki, H., Yamanishi, H., & Koga, K. (2006). Salinization processes in an alluvial coastal lowland plain and effect of sea water level rise. *Environmental Geology*, *49*(5), 743–751. https://doi.org/10.1007/s00254-005-0119-7

Dörr, N., Schenk, A., & Hinz, S. (2021). Analysis of heterogeneous Ps-InSAR derived subsidence rates using categorized Gis objects - A case study in the Mekong Delta. In *International Geoscience and Remote Sensing Symposium (IGARSS)* (pp. 2655–2658). https://doi.org/10.1109/IGARSS47720.2021.9553297

Dörr, N., Schenk, A., & Hinz, S. (2024a). Land subsidence in the Mekong Delta derived from advanced persistent scatterer interferometry with an infrastructural reference network. *IEEE Journal of Selected Topics in Applied Earth Observations and Remote Sensing*, *17*, 12077–12091. https://doi.org/10.1109/JSTARS.2024.3420130

Dörr, N., Schenk, A., & Hinz, S. (2024b). Vertical surface displacement time series in the Vietnamese Mekong Delta derived from advanced Sentinel-1 persistent scatterer interferometry [Dataset]. *Karlsruhe Institute of Technology*. https://doi.org/10.35097/YYpQiWnfZaqMVybS

Erban, L. E., Gorelick, S. M., & Zebker, H. A. (2014). Groundwater extraction, land subsidence, and sea-level rise in the Mekong Delta, Vietnam. *Environmental Research Letters*, *9*(8), 084010. https://doi.org/10.1088/1748-9326/9/8/084010

Haghighi, M. H., & Motagh, M. (2024). Uncovering the impacts of depleting aquifers: A remote sensing analysis of land subsidence in Iran. *Science Advances*, *10*(19), 1–11. https://doi.org/10.1126/sciadv.adk3039

Käkönen, M. (2008). Mekong Delta at the crossroads: More control or adaptation? *Ambio: A Journal of the Human Environment*, *37*(3), 205–212. https://doi.org/10.1579/0044-7447(2008)37[205:MDATCM]2.0.CO;2

Karlsrud, K., Tunbridge, L., Khanh, N. Q., & Dinh, N. Q. (2020). Preliminary results of land subsidence monitoring in the Ca Mau Province. *Proceedings of the International Association of Hydrological Sciences*, *382*, 111–115. https://doi.org/10.5194/piahs-382-111-2020

Kaveney, B., Barrett-Lennard, E., Chau Minh, K., Dang Duy, M., Nguyen Thi, K. P., Kristiansen, P., et al. (2023). Inland dry season saline intrusion in the Vietnamese Mekong River Delta is driving the identification and implementation of alternative crops to rice. *Agricultural Systems*, *207*(August 2022), 103632. https://doi.org/10.1016/j.agsy.2023.103632

Keetch, J. J., & Byram, G. M. (1968). *A drought index for forest fire control* (Vol. 38). US Department of Agriculture, Forest Service, Southeastern Forest Experiment Station.

Kondolf, G. M., Schmitt, R. J., Carling, P. A., Goichot, M., Keskinen, M., Arias, M. E., et al. (2022). Save the Mekong Delta from drowning. *Science*, *376*(6593), 583–585. https://doi.org/10.1126/science.abm5176

Kumiko, T., Takao, M., & Toru, M. (2008). Seasonal changes in radiation and evaporation implied from the diurnal distribution of rainfall in the Lower Mekong. *Hydrological Processes*, *22*(9), 1257–1266. https://doi.org/10.1002/hyp.6935

Lavane, K., Kumar, P., Meraj, G., Han, T. G., Ngan, L. H. B., Lien, B. T. B., et al. (2023). Assessing the effects of drought on rice yields in the Mekong Delta. *Climate*, *11*(1), 13. https://doi.org/10.3390/cli11010013

Loc, H. H., Low Lixian, M., Park, E., Dung, T. D., Shrestha, S., & Yoon, Y. J. (2021). How the saline water intrusion has reshaped the agricultural landscape of the Vietnamese Mekong Delta, a review. *Science of the Total Environment*, *794*, 148651. https://doi.org/10.1016/j.scitotenv.2021.148651

Loc, H. H., Van Binh, D., Park, E., Shrestha, S., Dung, T. D., Son, V. H., et al. (2021). Intensifying saline water intrusion and drought in the Mekong Delta: From physical evidence to policy outlooks. *Science of the Total Environment*, *757*, 143919. https://doi.org/10.1016/j.scitotenv.2020.143919

Miller, M. M., Jones, C. E., Sangha, S. S., & Bekaert, D. P. (2020). Rapid drought-induced land subsidence and its impact on the California aqueduct. *Remote Sensing of Environment*, *251*(August), 112063. https://doi.org/10.1016/j.rse.2020.112063

Miller, M. M., & Shirzaei, M. (2019). Land subsidence in Houston correlated with flooding from Hurricane Harvey. *Remote Sensing of Environment*, *225*, 368–378. https://doi.org/10.1016/j.rse.2019.03.022

Mills, B., Le, D. P., Ta, D. P., Nhu, L., Vo, D. T., & Labarta, R. (2023). Intensive and extensive rice farm adaptations in salinity-prone areas of the Mekong Delta. *Climate & Development*, *15*(2), 162–176. https://doi.org/10.1080/17565529.2022.2072800

Minderhoud, P. S., Coumou, L., Erkens, G., Middelkoop, H., & Stouthamer, E. (2019). Mekong Delta much lower than previously assumed in sea-level rise impact assessments. *Nature Communications*, *10*(1), 1–13. https://doi.org/10.1038/s41467-019-11602-1

Minderhoud, P. S., Erkens, G., Pham, V. H., Bui, V. T., Erban, L., Kooi, H., & Stouthamer, E. (2017). Impacts of 25 years of groundwater extraction on subsidence in the Mekong Delta, Vietnam. *Environmental Research Letters*, *12*(6), 064006. https://doi.org/10.1088/1748-9326/aa7146

Minderhoud, P. S., Hlavacova, I., Kolomaznik, J., & Neussner, O. (2020). Towards unraveling total subsidence of a mega-delta-the potential of new PS InSAR data for the Mekong Delta. *Proceedings of the International Association of Hydrological Sciences*, *382*, 327–332. https://doi.org/10.5194/piahs-382-327-2020

Minderhoud, P. S., Middelkoop, H., Erkens, G., & Stouthamer, E. (2020). Groundwater extraction may drown mega-delta: Projections of extraction-induced subsidence and elevation of the Mekong Delta for the 21st century. *Environmental Research Communications*, *2*(1), 011005. https://doi.org/10.1088/2515-7620/ab5e21

Minderhoud, P. S., Shirzaei, M., & Teatini, P. (2025). From InSAR-derived subsidence to relative sea-level rise—A call for rigor. *Earth's Future*, *13*(1), e2024EF005539. https://doi.org/10.1029/2024EF005539

Muñoz Sabater, J., Comyn-Platt, E., Hersbach, H., Bell, B., Berrisford, P., Biavati, G., et al. (2024). ERA5-land post-processed daily-statistics from 1950 to present [Dataset]. *Copernicus Climate Change Service (C3S) Climate Data Store (CDS)*. https://doi.org/10.24381/cds.e9c9c792

Ojha, C., Shirzaei, M., Werth, S., Argus, D. F., & Farr, T. G. (2018). Sustained groundwater loss in California's central valley exacerbated by intense drought periods. *Water Resources Research*, *54*(7), 4449–4460. https://doi.org/10.1029/2017WR022250

Smajgl, A., Toan, T. Q., Nhan, D. K., Ward, J., Trung, N. H., Tri, L. Q., et al. (2015). Responding to rising sea levels in the Mekong Delta. *Nature Climate Change*, *5*(2), 167–174. https://doi.org/10.1038/nclimate2469

Stewart, R. D., Rupp, D. E., Abou Najm, M. R., & Selker, J. S. (2016). A unified model for soil shrinkage, subsidence, and cracking. *Vadose Zone Journal*, *15*(3), 1–15. https://doi.org/10.2136/vzj2015.11.0146

Syvitski, J. P., Kettner, A. J., Overeem, I., Hutton, E. W., Hannon, M. T., Brakenridge, G. R., et al. (2009). Sinking deltas due to human activities. *Nature Geoscience*, *2*(10), 681–686. https://doi.org/10.1038/ngeo629

Takeuchi, W., Darmawan, S., Shofiyati, R., Khiem, M. V., Oo, K. S., Pimple, U., & Heng, S. (2015). Near-real time meteorological drought monitoring and early warning system for croplands in Asia. In *ACRS 2015 - 36th Asian conference on remote sensing: Fostering resilient growth in Asia, Proceedings*.

Tellman, B., Sullivan, J. A., Kuhn, C., Kettner, A. J., Doyle, C. S., Brakenridge, G. R., et al. (2021). Satellite imaging reveals increased proportion of population exposed to floods. *Nature*, *596*(7870), 80–86. https://doi.org/10.1038/s41586-021-03695-w

Trung, N. H., Woillez, M.-N., Thanh, N. D., Eslami, S., Minderhoud, P., Quan, T. A., et al. (2021). Chapter 7 The Mekong Delta in the face of increasing climatic and anthropogenic pressures. In *Climate change in Viet Nam: Impacts and adaptation* (pp. 339–369).

Van Loon, A. F., Gleeson, T., Clark, J., Van Dijk, A. I., Stahl, K., Hannaford, J., et al. (2016). Drought in the anthropocene. *Nature Geoscience*, *9*(2), 89–91. https://doi.org/10.1038/ngeo2646

Wagner, F., Tran, V. B., & Renaud, F. G. (2012). Groundwater resources in the Mekong Delta: Availability, utilization and risks. In *The Mekong Delta System (Md)* (pp. 201–220). https://doi.org/10.1007/978-94-007-3962-8_7

Wehrheim, C., Lübken, M., Stolpe, H., & Wichern, M. (2023). Identifying key influences on surface water quality in freshwater areas of the Vietnamese Mekong Delta from 2018 to 2020. *Water (Switzerland)*, *15*(7), 1295. https://doi.org/10.3390/w15071295

Welch, J., Wang, G., Bao, Y., Zhang, S., Huang, G., & Hu, X. (2024). Unveiling the hidden threat: Drought-induced inelastic subsidence in expansive soils. *Geophysical Research Letters*, *51*(7), e2023GL107549. https://doi.org/10.1029/2023GL107549

Yoon, J. H., Simon Wang, S. Y., Gillies, R. R., Hipps, L., Kravitz, B., & Rasch, P. J. (2015). Extreme fire season in California: A glimpse into the future? *Bulletin of the American Meteorological Society*, *96*(12), S5–S9. https://doi.org/10.1175/BAMS-D-15-00114.1

Zoccarato, C., Minderhoud, P. S., & Teatini, P. (2018). The role of sedimentation and natural compaction in a prograding delta: Insights from the mega Mekong Delta, Vietnam. *Scientific Reports*, *8*(1), 1–12. https://doi.org/10.1038/s41598-018-29734-7

Zou, L., Kent, J., Lam, N. S., Cai, H., Qiang, Y., & Li, K. (2016). Evaluating land subsidence rates and their implications for land loss in the Lower Mississippi River Basin. *Water (Switzerland)*, *8*(1), 1–15. https://doi.org/10.3390/w8010010